IET Nanobiotechnology

The Institution of Engineering and Technology WILEY

ORIGINAL RESEARCH

Drug delivery and anticancer activity of biosynthesised mesoporous Fe_2O_3 nanoparticles

Firoozeh Abolhasani Zadeh[1] | Saade Abdalkareem Jasim[2] | Nigora E. Atakhanova[3] | Hasan Sh. Majdi[4] | Mohammed Abed Jawad[5] | Mohammed Khudair Hasan[6] | Fariba Borhani[7] | Mehrdad Khatami[8]

[1]Department of Surgery, Faculty of Medicine, Kerman University of Medical Sciences, Kerman, Iran

[2]Medical Laboratory Techniques Department, Al-maarif University College, Al-anbar-Ramadi, Iraq

[3]Department of Oncology and Radiology, Tashkent Medical Academy, Tashkent, Uzbekistan

[4]Department of Chemical Engineering and Petroleum Industries, Al-Mustaqbal University College, Babylon, Iraq

[5]Al-Nisour University College, Baghdad, Iraq

[6]Department of Pharmacy, Al-Manara College of Medical Sciences, Missan, Iraq

[7]Medical Ethics and Law Research Center, Shahid Beheshti University of Medical Sciences, Tehran, Iran

[8]Department of Medical Biotechnology, Faculty of Medical Sciences, Tarbiat Modares University, Tehran, Iran

Correspondence

Fariba Borhani, Medical Ethics and Law Research Center, Shahid Beheshti University of Medical Sciences, Tehran, Iran.
Email: faribaborhani@msn.com

Mehrdad Khatami, Department of Medical Biotechnology, Faculty of Medical Sciences, Tarbiat Modares University, Tehran, Iran. Postal :19857-17443
Email: Mehrdad7khatami@gmail.com

Abstract

Mesoporous magnetic nanoparticles of haematite were synthesised using plant extracts according to bioethics principles. The structural, physical and chemical properties of mesoporous Fe_2O_3 nanoparticles synthesised with the green chemistry approach were evaluated by XRD, SEM, EDAX, BET, VSM and HRTEM analysis. Then, their toxicity against normal HUVECs and MCF7 cancer cells was evaluated by MTT assay for 48 h. These biogenic mesoporous magnetic nanoparticles have over 71% of doxorubicin loading efficiency, resulting in a 50% reduction of cancer cells at a 0.5 $\mu g.ml^{-1}$ concentration. Therefore, it is suggested that mesoporous magnetic nanoparticles be used as a multifunctional agent in medicine (therapeutic-diagnostic). The produced mesoporous magnetic nanoparticles with its inherent structural properties such as polygonal structure (increasing surface area to particle volume) and porosity with large pore volume became a suitable substrate for loading the anti-cancer drug doxorubicin.

KEYWORDS

bioethics principles, MCF-7 breast cancer cell line, mesoporous magnetic nanoparticles, MTT test, targeted transfer

1 | INTRODUCTION

Cancer is one of the most common diseases that affect many people worldwide [1]. Cancer is the uncontrolled growth of cells in the body that starts from a point in the body, and if diagnosed late, it can affect the whole body [2–5]. Cancer treatments are done to improve cancer's condition or stop its progression. Depending on the patient's condition, a treatment method or a combination of different treatments may be performed to improve the patient's disease [6]. Surgery and radiation therapy are common treatments. Killing cancer cells using chemotherapy [7], immunotherapy [8], hormone therapy [9] are among the drug treatments [10]. But one of the disadvantages of this method is that along with the destruction of

cancer cells, normal cells are targeted and destroyed [11]. Therefore, research and development of new cancer treatment methods are needed [12–14]. New developments in science and technology have significant impact on human health [15–29] and life [30–36].

Nanostructures have attracted much attention as a new diagnostic and therapeutic method [37–46]. Targeted delivery of nanomaterials and combination therapy with current cancer drugs are among the potential nanosystems in identifying and destroying cancer cells [47]. Nanosystems do not have the limitations of cancer treatments such as drug resistance, adverse side effects, and high treatment costs. Furthermore, mesoporous nanostructure has been evaluated due to the direct loading of the drug in their cavities and their targeted transport capability [48, 49].

Considering their special physicochemical properties, nanoparticles have attracted much attention in treatment and diagnosis [50–54] such as Coronavirus disease 19 (COVID-19) [55–58], which is very contagious and has quickly spread around the world [59–65]. Various studies have been conducted on the application of iron nanoparticles in medicine. Nosrati et al. coated the Fe_3O_4 nanoparticles with lysine and then loaded the drug methotrexate [66]. They showed that the toxicity of loaded nanoparticles against MCF7 cancer cells was higher than that of high magnetite nanoparticles. In another study, small and high concentrations of iron nanoparticles caused mitochondrial damage and increased apoptosis in MCF7 cancer cells [67]. Alarifi et al. showed that combining the anti-cancer drug with Fe_2O_3 nanoparticles against breast cancer cells increased apoptosis [67]. Therefore, in this study, mesoporous iron nanoparticles were synthesised in one step with phenolic compounds of the plant. XRD investigated the physicochemical properties of these nanoparticles, SEM, HRTEM, and BET analyses. Then, the anti-cancer drug doxorubicin was loaded into pores of biosynthesised mesoporous nanoparticles. Finally, the toxicity of biosynthesised nanoparticles, loaded doxorubicin nanoparticles against normal HUVECs, and MCF7 cancer cells was evaluated with MTT assay.

2 | MATERIALS AND METHODS

2.1 | Biological synthesis of mesoporous Fe_2O_3 nanoparticles

The surface dust of healthy *Mentha piperita* leaves was washed with deionised water. Leaf surface moisture was removed in an oven at 40°C. Then, 7 ml of deionised water was added per 1 g of dried leaf powder and shaken at 37°C for 24 h. 4 g of iron (III) nitrate nano-hydrate (Sigma-Aldrich, Fe $(NO_3)_3$ $9H_2O \geq 98\%$) was added to 30 ml of extract at 10°C and completely dissolved with a strainer. Then, 15 ml of deionised water was added to the mixture and sterilised for 5 minutes, and then transferred to an autoclave and placed in an oven at 170°C for 13 h. The nanoparticles were then separated via centrifugation and calcined at 300°C for 3 h [68].

2.2 | Characterisation of mesoporous Fe_2O_3 nanoparticles

X-Ray Diffraction (XRD) analysis was performed using Panalytical's X'PertPro to detect the type of synthesised nanoparticles. XRD analysis was performed at 2θ from 10 to 80° using 1.54 Å X-ray wavelength. Scanning electron microscope (SEM) analysis was performed to determine the morphology of the nanoparticles and identify chemical compounds using Sigma VP device, ZEISS Company. High-resolution transmission electron microscopy (HRTEM) and Brunauer–Emmett–Teller (BET) analyses were used to determine the microstructural properties and investigate the synthesised nanoparticles' surface porosity. HRTEM analysis was performed using a device (Tecnai 20, FEI Company), and BET analysis was performed using a device (Belsorp mini II, Microtrac Bel Corp Company). The synthesised nanoparticles were degassed for BET analysis. Magnetic properties of the synthesised nanoparticles were determined using vibrating-sample magnetometer (VSM) analysis and Lake Shore Model 7400 [35, 36].

2.3 | Loading of doxorubicin to mesoporous Fe_2O_3 nanoparticles

0.01 g of mesoporous nanoparticles was added to 5 ccs of deionised water and then dispersed using an ultrasonic bath. The nanoparticle suspension was added to a 5 ml stock of 2 M doxorubicin (Sigma-Aldrich, $C_{27}H_{29}NO_{11}$) and sterilised overnight. The nanoparticles loaded with doxorubicin were then measured at 480 nm.

2.4 | Cytotoxic assessment of mesoporous Fe_2O_3 nanoparticles

Toxicity of doxorubicin, mesoporous Fe_2O_3 nanoparticles, doxorubicin-loaded mesoporous Fe_2O_3 nanoparticles against umbilical vein endothelial cells (HUVEC, normal cell), and MCF7 cancer cells was evaluated by MTT assay for 48 h. Cells in the culture medium containing 10% Foetal bovine serum (FBS, Sigma–Aldrich, USA), 1% streptomycin/penicillin antibiotic (100 µg.ml^{-1} streptomycin and 100 U/ml penicillin, GIBCO, UK), and 89% Dulbecco's Modified Eagle's Medium (DMEM; GIBCO Invitrogen, Paisley, UK) were cultured with high glucose at 37°C and 5% CO_2. 24 h after culturing the cells in 96 well containers (ELISA plate), in a repeated randomised design, and after changing the culture medium, cancer cells and normal cells with different concentrations of doxorubicin, mesoporous Fe_2O_3 nanoparticles, and doxorubicin-loaded mesoporous Fe_2O_3 nanoparticles were treated and incubated for 48 h. The cells were then washed with phosphate-buffered saline buffer (PBS, Sigma–Aldrich, USA) and discarded. Then, 10 µl of dye 3-(4,5-Dimethylthiazol-2-yl) −2,5-diphenyltetrazolium bromide (MTT, Sigma-Aldrich, USA) (5 mg.ml^{-1} in PBS)
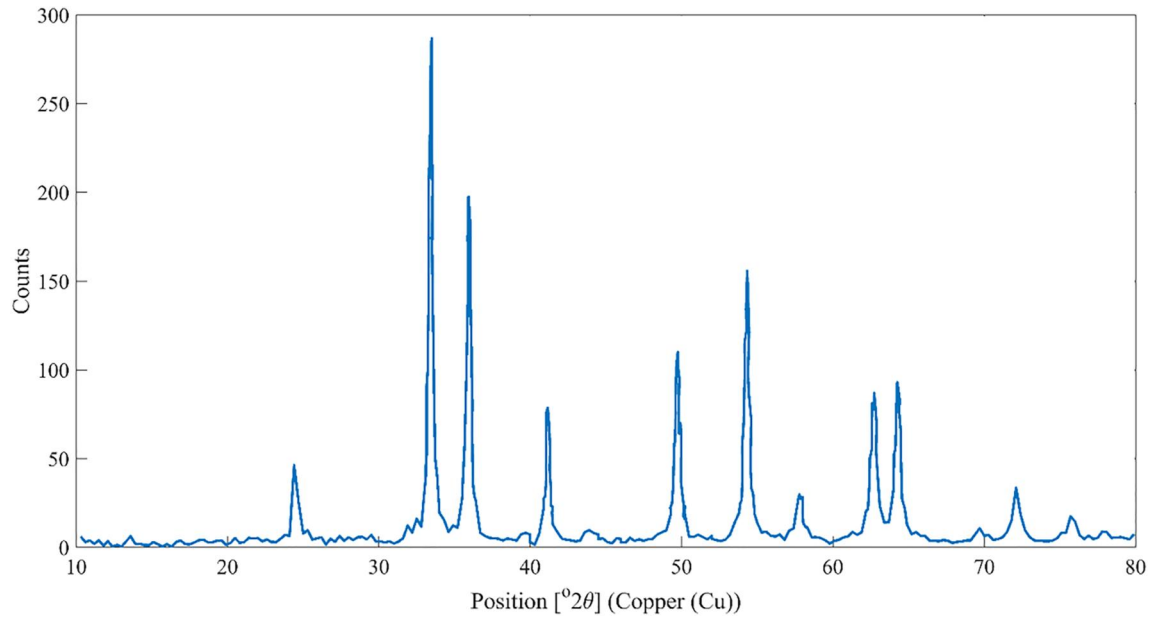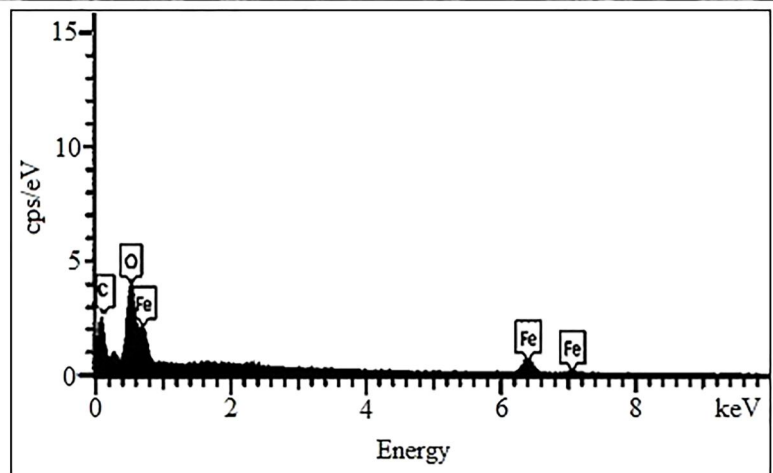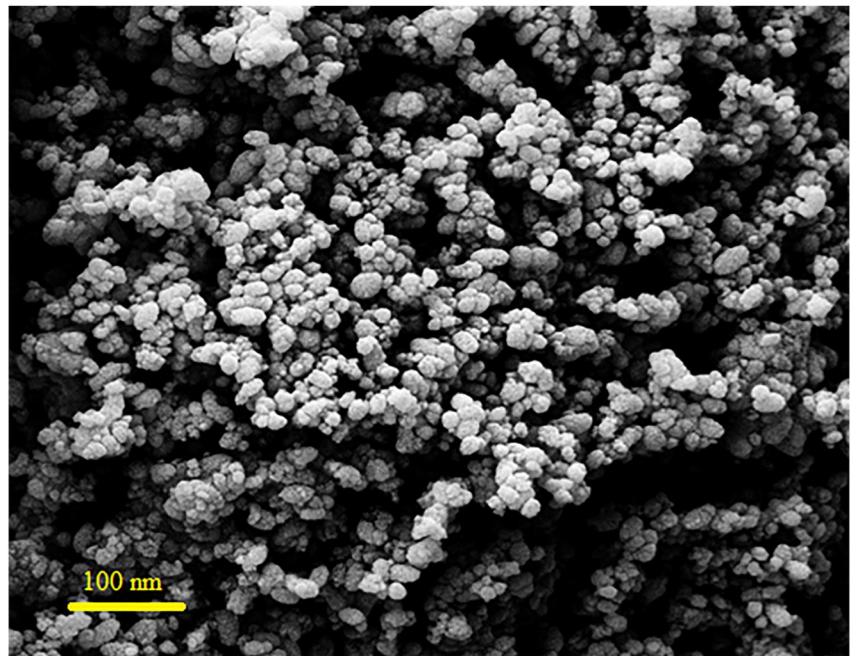
FIGURE 1 X-Ray Diffraction (XRD) pattern of mesoporous Fe_2O_3 nanoparticles synthesised using plant extract

FIGURE 2 SEM-EDAX micrograph of mesoporous Fe_2O_3 nanoparticles

was applied to each well. The plate was incubated at 37°C with 5% CO2 for 3 h. The MTT medium was extracted, and the formazan crystals were dissolved by adding 100 μl (DMSO (CH3)2SO, Sigma–Aldrich) dimethyl sulfoxide to each well of the plate and then stored in a dark place at 25°C for 15 min. Finally, the absorption of soluble formazan at 570 nm (DYNEX MRX) was measured using a microplate reader [69].

3 | RESULTS AND DISCUSSION

The XRD diagram of mesoporous Fe_2O_3 nanoparticles synthesised using plant extract is shown in Figure 1. The peaks observed in the diagram confirm the structure of Fe_2O_3 haematite. Synthesised nanoparticles are free of impurities. The single-phase nature in synthesised nanoparticles and the sharp peaks in the XRD pattern are due to the calcination of the nanoparticles.

Figure 2 shows the surface morphology of mesoporous Fe_2O_3 nanoparticles. The synthesised mesoporous Fe_2O_3 nanoparticles have a spherical morphology. The EDAX micrograph confirms the presence of iron, oxygen, and carbon. The carbon elements in the synthesised mesoporous Fe_2O_3 nanoparticles structure demonstrate organic matter in the plant extract.

The synthesised mesoporous Fe_2O_3 nanoparticle's size and shape with a bright-field background is shown in Figure 3. The micrograph confirms the synthesised mesoporous Fe_2O_3 nanoparticles.
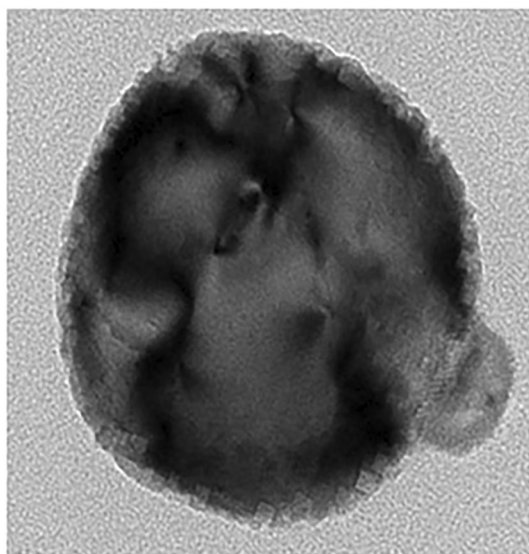
The BET analysis results are shown in Table 1. The average pore diameters and specific surface area of mesoporous Fe_2O_3 nanoparticles are 17.9 nm and 30 m^2 g^{-1}, respectively. According to the IUPAC classification of nitrogen uptake and desorption curves, these data confirm the presence of porosity in the nanoparticles, which is consistent with the HRTEM results (Figure 4). Hysteresis 3 confirms non-hard, plate-like porosity [16].

Magnetic behaviour of synthesised nanoparticles at room temperature and in a magnetic field $-20,000 \leq H$ (Oe) $\leq 20,000$ is shown in Figure 5. The VSM curve confirms the ferromagnetic properties of mesoporous Fe_2O_3 nanoparticles. Mesoporous Fe_2O_3 nanoparticles have a magnetic saturation of 0.6 emu/g.

In drug delivery reviews, drug loading is a separate and essential step. At this stage, various biocompatible polymers are used to load the drug on the surface of nanoparticles. In this study, the inherent porosity of mesoporous Fe_2O_3 nanoparticles made the loading of the anti-cancer drug doxorubicin without the coating polymer easy and inexpensive. To confirm the loading of the anti-cancer drug by synthesised mesoporous Fe_2O_3 nanoparticles, UV–vis spectroscopy analysis was performed on doxorubicin, mesoporous Fe_2O_3 nanoparticles, and mesoporous Fe_2O_3 nanoparticles loaded with doxorubicin. As shown in the figure, mesoporous Fe_2O_3 nanoparticles showed strong light absorption in the range of 520 nm. The displacement of the peak to the 475 nm region in the loaded mesoporous Fe_2O_3 nanoparticles spectrum confirms the dielectric bonding of the mesoporous Fe_2O_3 nanoparticles with doxorubicin. Also, mesoporous Fe_2O_3 nanoparticles with a loading efficiency of 70% are a new carrier in concert therapy.
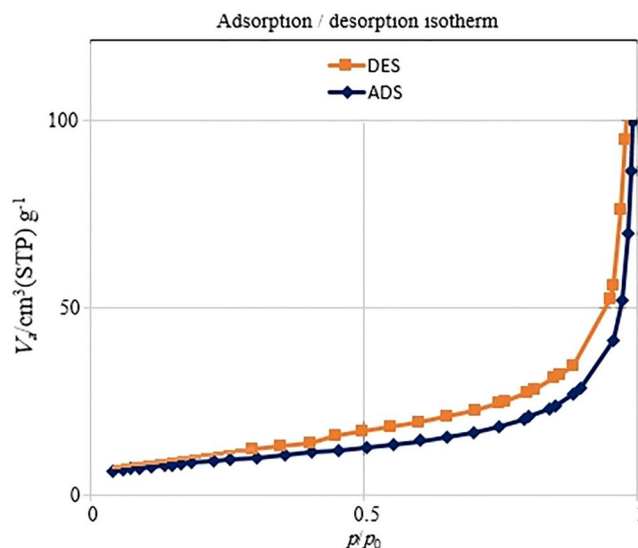

FIGURE 3 High-resolution transmission electron microscopy (HRTEM) micrograph of mesoporous Fe_2O_3 nanoparticles

FIGURE 4 Nitrogen adsorption–desorption isotherms of mesoporous Fe_2O_3 nanoparticles

Nanoparticles	BET surface area m^2/g^{-1}	Pore volume cm^3g^{-1}	Pore size nm
Fe_2O_3	30	0.1	18 ± 0.2

TABLE 1 Specific surface area (Brunauer–Emmett–Teller [BET]) of mesoporous Fe_2O_3 nanoparticles

This study evaluated the toxicity of mesoporous Fe_2O_3 nanoparticles and drug-loaded mesoporous Fe_2O_3 ones against MCF7 cancer cells and HUVECs normal cells with MTT assay. According to Figure 6, mesoporous Fe_2O_3 nanoparticles are less toxic to normal HUVECs and MCF7 cancer cells than doxorubicin. As a result, synthesised nanoparticles with low toxicity are considered safe for the body cells. The toxicity of doxorubicin-loaded mesoporous Fe_2O_3 nanoparticles on normal HUVECs cells at a 1 $\mu g.ml^{-1}$ concentration is negligible and, with increasing attention, has high toxicity on normal cells the body. Also, mesoporous Fe_2O_3 nanoparticles loaded with doxorubicin at a 0.5 $\mu g.ml^{-1}$ concentration reduced MCF7 cancer cells by 50%. As shown in Figure 6, there is a significant difference between the toxicity of doxorubicin and doxorubicin-loaded mesoporous Fe_2O_3 nanoparticles.

Based on XRD, TEM, and BET data, the rhombic and hexagonal crystal structure with good porosity has resulted in the high loading of biogenic mesoporous Fe_2O_3 nanoparticles. In addition, the polygonal structure of these nanoparticles has increased the surface area to particle volume, which has been critical in the optimal loading of doxorubicin. Despite the safe nature of mesoporous Fe_2O_3 nanoparticles, a good result was obtained in MTT evaluations. Therefore, the use of mesoporous Fe_2O_3 nanoparticles in drug/gene delivery creates a great revolution. Their special advantages as mesopores with large pore volume and their purposeful control due to their magnetic properties make them nanosystems for diagnosis and treatment. As mentioned, due to the presence of plant organic matter in the nanocarrier structure, these particles are not very toxic to cancer cells. Therefore, to use the synergistic effect of nanoparticle toxicity and anti-cancer drug toxicity, it is recommended to use mesoporous Fe_2O_3 nanoparticles in drug delivery.
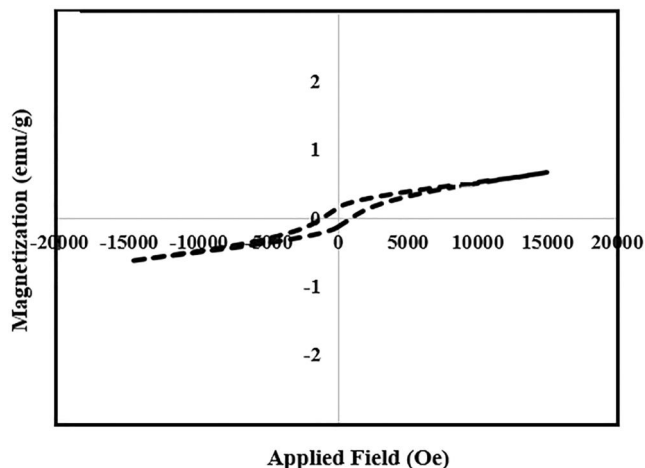

FIGURE 5 Vibrating-sample magnetometer (VSM) curve of mesoporous Fe_2O_3 nanoparticles
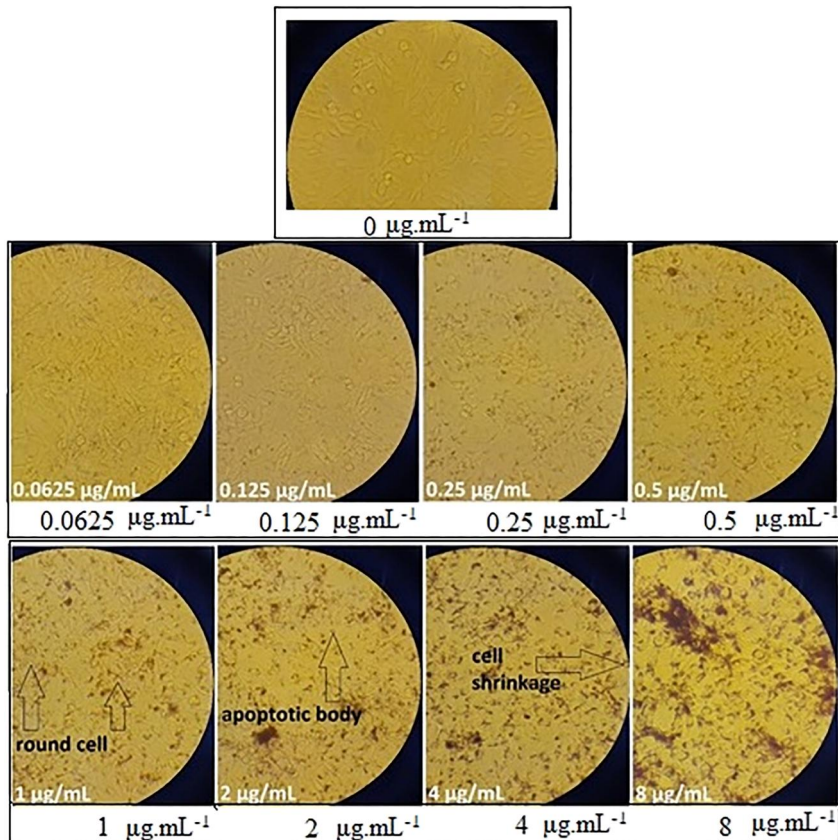

FIGURE 6 Cytotoxic effects of mesoporous Fe_2O_3 nanoparticles, DOX, and DOX-loaded mesoporous Fe_2O_3 nanoparticles against MCF7 and HUVECs cell lines (* p-value < 0.01)

4 | CONCLUSION

In this study, haematite mesoporous Fe_2O_3 nanoparticles were synthesised in one step by the green chemistry method. Production of mesoporous Fe_2O_3 nanoparticles is of low-cost and centuries-old due to its porosity nature and green chemistry method. Also, the manufactured nanoparticles have low toxicity on normal cells of the body, so they are considered safe drug carriers in treatment and diagnosis. The toxicity of doxorubicin-loaded mesoporous Fe_2O_3 nanoparticles on breast cancer cells at low concentrations is important as a new therapeutic agent.

CONFLICT OF INTEREST
The authors confirm that there are no conflict of interest.

PERMISSION TO REPRODUCE MATERIALS FROM OTHER SOURCES
None.

DATA AVAILABILITY STATEMENT
The data that support the findings of this study are available on request from the corresponding author. The data are not publicly available due to privacy or ethical restrictions.

ORCID
Mehrdad Khatami https://orcid.org/0000-0002-7519-6998

REFERENCES

1. Beyzadeoglu, M., Ozyigit, G., Ebruli, C.: Genitourinary system cancers', *basic radiation Oncology*. Springer (2022)
2. Subash, A., et al.: Oral cancer in India, a growing problem: is limiting the exposure to avoidable risk factors the only way to reduce the disease burden? Oral Oncol. 125, 105677 (2022)
3. Feng, Y., et al.: Pan-cancer analysis and experiments with cell lines reveal that the slightly elevated expression of Dlgap5 is involved in clear cell renal cell carcinoma progression. Life Sci. 287, 120056 (2021)
4. Islam, M., et al.: Study on mitochondrial Atpase6 gene polymorphisms as a genetic risk factor for breast cancer in Bangladeshi women. Int. J. Scientific Res. Dental Medical Sci. 3(1), 18–22 (2021)
5. Dinita Devi, N., et al.: Askin tumor: a case report of a rare tumor. Int. J. Scientific Res. Dental Medical Sci. 3(3), 153–155 (2021)
6. Zheng, J.W., et al.: Guidelines for the treatment of head and neck venous malformations. Int. J. Clin. Exp. Med. 6(5), 377 (2013)
7. Sartaj, A., Baboota, S., Ali, J.: Assessment of combination approaches of phytoconstituents with chemotherapy for the treatment of breast cancer, a systematic review. Curr. Pharmaceut. Des. (2021)
8. Reck, M., Remon, J., Hellmann, M.D.: First-line immunotherapy for non–small-cell lung cancer. J. Clin. Oncol. 21, 01497 (2022)
9. Geraghty, P.: Menopause hormone therapy, Each Woman's Menopause: An Evidence Based Resource. Springer (2022)
10. Billy, F., Clairambault, J., Fercoq, O.: Optimisation of cancer drug treatments using cell population dynamics, Mathematical Methods Models Biomedicine. Springer (2013)
11. Chang, K.: Targeted cancer therapy—an evolving approach for cancer treatment. Humanities (2022)
12. Miri, A., et al.: Photocatalytic performance and cytotoxic activity of green-synthesized cobalt ferrite nanoparticles. Mater. Res. Bull. 149, 111706 (2022)
13. Cao, Y., et al.: Ceramic magnetic ferrite nanoribbons: eco-friendly synthesis and their antifungal and parasiticidal activity. Ceram. Int. (2021)
14. Cao, Y., et al.: Green synthesis of bimetallic zno–cuo nanoparticles and their cytotoxicity properties. Sci. Rep. 11(1), 1–8 (2021)
15. Zha, T.-H., et al., pp. 160–176. A fuzzy-based strategy to suppress the novel Coronavirus (2019-ncov) massive outbreak. Applied and Computational Mathematics (2021)
16. Nazeer, M., et al.: Theoretical study of mhd electro-osmotically flow of third-grade fluid in micro channel. Appl. Math. Comput. 420, 126868 (2022)
17. Zhao, T.H., Khan, M.I., Chu, Y.M.: Artificial neural networking (ann) analysis for heat and entropy generation in flow of non-Newtonian fluid between two rotating disks. Math. Methods Appl. Sci. (2021)
18. Song, Y.-Q., et al.: Optimal evaluation of a toader-type mean by power mean. J. Inequalities Appl. 2015(1), 1–12 (2015)
19. Zhao, T.-H., Qian, W.-M., Chu, Y.-M.: Sharp power mean bounds for the tangent and hyperbolic sine means. J. Math. Inequalities. 15(4), 1459–1472 (2021)
20. Wang, F., et al.: Numerical solution of traveling waves in chemical kinetics: time fractional Fishers equations. Fractals (2021)
21. Delavari, S., et al.: Development and psychometrics of script concordance test (Sct) in midwifery. Med. J. Islam. Repub. Iran. 32, 75 (2018)
22. Sohrabi, Z., et al.: The effects of group blogging on the attitude towards virtual education in nursing students. Med. J. Islam. Repub. Iran. 31, 132 (2017)
23. Ramezani, G., et al.: Comparing peer education with tbl workshop in (ebm) teaching. Med. J. Islam. Repub. Iran. 34, 70 (2020)
24. Fathi, A., Giti, R., Farzin, M.: How different influential factors affect the color and translucency of Y-ztp: a review of the literature. Ann. Dent. Spec. 6(3), 338–341 (2018)
25. Fathi, A., et al.: Effects of number of firings and veneer thickness on the color and translucency of 2 different zirconia-based ceramic systems. J. Prosthet. Dent. 122(6), 565 e561–565 e567 (2019)
26. Ghasemi, E., Fathi, A.H., Parvizinia, S.: Effect of three disinfectants on dimensional changes of different impression materials. J. Iranian Dental Assoc. 31(3), 169–176 (2019)
27. Monirifard, R., et al.: Relationship of personality traits and patient satisfaction with fixed implant prosthodontic treatments. J. Iranian Dental Assoc. 31(4), 182–188 (2019)
28. Ebadian, B., Fathi, A., Khodadad, S.: Comparison of the effect of four different abutment screw torques on screw loosening in single implant-supported prosthesis after the application of mechanical loading. Int. J. Dentistry, 2021 (2021)
29. Ebadian, B., Fathi, A., Savoj, M.: In vitro evaluation of the effect of different luting cements and tooth preparation angle on the microleakage of zirconia crowns. Int. J. Dentistry, 2021 (2021)
30. Barakati, T., et al.: Evaluate the effect of various titanium abutment modifications on the behavior of peri-implant soft tissue healing, inflammation, and maintenance: a systematic review and meta-analysis. Turkish Online J. Qual. Inquiry. 12(7), 11401–11410 (2021)
31. Ashtiani, A.H., Mardasi, N., Fathi, A.: Effect of multiple firings on the shear bond strength of presintered cobalt-chromium alloy and veneering ceramic. J. Prosthet. Dent. 126(6), 803 e801–803 e806 (2021)
32. Mosharraf, R., et al.: Investigating the effect of nonrigid connectors on the success of tooth-and-implant-supported fixed partial prostheses in maxillary anterior region: a finite element analysis (fea). Int. J. Dentistry, 2021 (2021)
33. Abolhasani, M., et al.: Color change of ceramill zolid fx following abrasion with/without toothpaste. J. Iranian Dental Assoc. 33(3), 51–57 (2021)
34. Maalekipour, M., et al.: Effect of adhesive resin as a modeling liquid on elution of resin composite restorations. Int. J. Dentistry, 2021 (2021)
35. Fathi, A., Salehi, A.: Antimicrobial resistance properties of Helicobacter pylori strains isolated from dental plaque and saliva samples. Academic J. Health Sci.: Medicina balear. 37(1), 29–33 (2022)

36. Khamisi, N., Fathi, A., Yari, A.: Antimicrobial resistance of Staphylococcus aureus isolated from dental plaques. Academic J. Health Sci.: Medicina balear. 37(1), 136–140 (2022)

37. Salarpour, S., et al.: The application of exosomes and exosome-nanoparticle in treating brain disorders. J. Mol. Liq. 350, 118549 (2022)

38. Rajaei, M., et al.: Sensitive detection of morphine in the presence of dopamine with La3+ doped fern-like cuo nanoleaves/mwcnts modified carbon paste electrode. J. Mol. Liq. 284, 462–472 (2019)

39. Jaleh, B., et al.: Laser-assisted preparation of Pd nanoparticles on carbon cloth for the degradation of environmental pollutants in aqueous medium. Chemosphere. 246, 125755 (2020)

40. Nazari-Vanani, R., Heli, H., Sattarahmady, N.: An impedimetric genosensor for leishmania infantum based on electrodeposited cadmium sulfide nanosheets. Talanta. 217, 121080 (2020)

41. Heli, H., et al.: Electrocatalytic oxidation of the antiviral drug acyclovir on a copper nanoparticles-modified carbon paste electrode. J. Solid State Electrochem. 14(5), 787–795 (2010)

42. Shafiee, A., et al.: Core–shell nanophotocatalysts: review of materials and applications. ACS Applied Nano Materials (2022)

43. Bai, X., et al.: Experimental evaluation of the lubrication performances of different nanofluids for minimum quantity lubrication (mql) in milling Ti-6al-4v. Int. J. Adv. Manuf. Technol. 101(9), 2621–2632 (2019)

44. Jia, D., et al.: Experimental verification of nanoparticle jet minimum quantity lubrication effectiveness in grinding. J. Nanoparticle Res. 16(12), 1–15 (2014)

45. Chu, Y.-M., et al.: Combined impact of cattaneo-christov double diffusion and radiative heat flux on bio-convective flow of maxwell liquid configured by a stretched nano-material surface. Appl. Math. Comput. 419, 126883 (2022)

46. Chu, Y.-M., et al.: Enhancement in thermal energy and solute particles using hybrid nanoparticles by engaging activation energy and chemical reaction over a parabolic surface via finite element approach. Fractal and Fractional. 5(3), 119 (2021)

47. Rahdar, A., et al.: Lignin-stabilized doxorubicin microemulsions: synthesis, physical characterization, and in vitro assessments. Polymers. 13(4), 641 (2021)

48. Torkzadeh-Mahani, M., et al.: A combined theoretical and experimental study to improve the thermal stability of recombinant D-lactate dehydrogenase immobilized on a novel superparamagnetic Fe3o4nps@Metal–organic framework. Appl. Organomet. Chem. 34(5), e5581 (2020)

49. Lai, W.-F., Huang, E., Lui, K.-H.: Alginate-based complex fibers with the janus morphology for controlled release of Co-delivered drugs. Asian J. Pharm. Sci. 16(1), 77–85 (2021)

50. Sargazi, S., et al.: Assessment of Snfe2o4 nanoparticles for potential application in theranostics: synthesis, characterization, in vitro, and in vivo toxicity. Materials. 14(4), 825 (2021)

51. Huang, B., et al.: Advances in fabrication of ceramic corundum abrasives based on sol–gel process. Chin. J. Aeronaut. 34(6), 1–17 (2021)

52. Yang, M., et al.: Predictive Model of convective heat transfer coefficient in bone micro-grinding using nanofluid aerosol cooling. Int. Commun. Heat Mass Tran. 125, 105317 (2021)

53. Yin, Q., et al.: Effects of physicochemical properties of different base oils on friction coefficient and surface roughness in mql milling aisi 1045. Int. J. Precision Eng. Manufacturing Green Technol., 1–19 (2021)

54. Zhang, J., et al.: Experimental assessment of an environmentally friendly grinding process using nanofluid minimum quantity lubrication with cryogenic air. J. Clean. Prod. 193, 236–248 (2018)

55. Rabiee, N., et al.: Quantum dots against Sars-cov-2: diagnostic and therapeutic potentials. J. Chem. Technol. Biotechnol. n/a(n/a)

56. Aslam, N., Ahmed, A.: Prospective impact of covid-19 on adolescents: guidelines for interventions. Psychiatr. Danub. 32(3-4), 603–604 (2020)

57. Amici, P.: Humor in the age of covid-19 lockdown: an explorative qualitative study. Psychiatr. Danub. 32(Suppl 1), 15–20 (2020)

58. Zhang, Z., et al.: Single-cell rna analysis reveals the potential risk of organ-specific cell types vulnerable to Sars-cov-2 infections. Comput. Biol. Med. 140, 105092 (2022)

59. Singha, A., et al.: The impact of metabolic syndrome on clinical outcome of covid-19 patients: a retrospective study. Int. J. Scientific Res. Dental Medical Sci. 3(4), 161–165 (2021)

60. Baghizadeh Fini, M., Seraj, B., Ghadimi, S.: Covid-19 in pediatric patients: a literature review. Int. J. Scientific Res. Dental Medical Sci. 2(4), 126–130 (2020)

61. Wei, F.F., et al.: Evaluating the treatment with favipiravir in patients infected by covid-19: a systematic review and meta-analysis. Int. J. Scientific Res. Dental Medical Sci. 2(3), 87–91 (2020)

62. Hirman, A.R., Murad, F.A., Nikzad, A.A.: Severe scabies after covid-19: a case report. Int. J. Scientific Res. Dental Medical Sci. 2(3), 97–100 (2020)

63. Casaroto, A.R., et al.: Evaluating epidemiology, symptoms, and routes of covid-19 for dental care: a literature review. Int. J. Scientific Res. Dental Medical Sci. 2(2), 37–41 (2020)

64. Aponte Mendez, M., et al.: Dental care for patients during the covid-19 outbreak: a literature review. Int. J. Scientific Res. Dental Medical Sci. 2(2), 42–45 (2020)

65. Jamali, S., et al.: Prevalence of malignancy and chronic obstructive pulmonary disease among patients with covid-19: a systematic review and meta-analysis. Int. J. Scientific Res. Dental Medical Sci. 2(2), 52–58 (2020)

66. Nosrati, H., et al.: Methotrexate-conjugated L-lysine coated iron oxide magnetic nanoparticles for inhibition of mcf-7 breast cancer cells. Drug Dev. Ind. Pharm. 44(6), 886–894 (2018)

67. Alarifi, S., et al.: Iron oxide nanoparticles induce oxidative stress, DNA damage, and caspase activation in the human breast cancer cell line. Biol. Trace Elem. Res. 159(1), 416–424 (2014)

68. Ansari, M.J., al, e.: Anticancer Drug-Loading Capacity of Green Synthesized Porous Magnetic Iron Nanocarrier and Cytotoxic Effects against Human Cancer Cell Line. J. Cluster Sci., 33, 1–8 (2022)

69. Al-Khedhairy, A.A., Wahab, R.: Silver Nanoparticles: An Instantaneous Solution for Anticancer Activity against Human Liver (Hepg2) and Breast (Mcf-7) Cancer Cells. Metals. 12(1), 148 (2022)